Chapter 19
Simulations of Galactic Dynamos

Axel Brandenburg

Abstract We review our current understanding of galactic dynamo theory, paying particular attention to numerical simulations both of the mean-field equations and the original three-dimensional equations relevant to describing the magnetic field evolution for a turbulent flow. We emphasize the theoretical difficulties in explaining non-axisymmetric magnetic fields in galaxies and discuss the observational basis for such results in terms of rotation measure analysis. Next, we discuss nonlinear theory, the role of magnetic helicity conservation and magnetic helicity fluxes. This leads to the possibility that galactic magnetic fields may be bi-helical, with opposite signs of helicity and large and small length scales. We discuss their observational signatures and close by discussing the possibilities of explaining the origin of primordial magnetic fields.

19.1 Introduction

We know that many galaxies harbor magnetic fields. They often have a large-scale spiral design (for a review, see the Chapter by Haverkorn in this volume). Understanding the nature of those fields was facilitated by an analogous problem in solar dynamo theory, where large-scale magnetic fields on the scale of the entire Sun were explained in terms of mean-field dynamo theory. Competing explanations in terms of primordial magnetic fields have been developed in both cases, but in solar dynamo theory there is the additional issue of an (approximately) cyclic variation, which is not easily explained in terms of primordial fields.

Historically, primordial magnetic fields were considered a serious contender in the explanation of the observed magnetic fields in our and other spiral galaxies; see the review of Sofue et al. (1986). The idea is simply that the differential rotation of the gas in galaxies winds up an ambient magnetic field to form a spiraling magnetic field pattern. There are two problems with this interpretation. Firstly, if there was no turbulent diffusion, the magnetic field would be wound up too many times to explain

A. Brandenburg (✉)
Nordic Institute for Theoretical Physics, KTH Royal Institute of Technology and Stockholm University, Roslagstullsbacken 23, 10691 Stockholm, Sweden
e-mail: brandenb@nordita.org

A. Lazarian et al. (eds.), *Magnetic Fields in Diffuse Media*, Astrophysics and Space Science Library 407, DOI 10.1007/978-3-662-44625-6_19

the observed field, whose magnetic spiral is not as tightly wound as one would have otherwise expected. The tight winding can be alleviated by turbulent diffusion, which is clearly a natural process that is expected to occur in any turbulent environment. In galaxies, an important source of turbulence is supernova explosions (Korpi et al. 1999; Gressel et al. 2008a; Gent et al. 2013a,b) that are believed to sustain the canonical values of a root-mean-square turbulent velocity of $u_{\rm rms} = 10\,{\rm km/s}$ at density $\rho = 2 \times 10^{-24}\,{\rm g\,cm^{-3}}$. The required vertically integrated energy input would be of the order of $0.5\rho u_{\rm rms}^3 \approx 10^{-24}\,{\rm g\,cm^{-3}}\,(10^6\,{\rm cm\,s^{-1}})^3 = 10^{-6}\,{\rm erg\,cm^{-2}\,s^{-1}}$. which is easily balanced by about 20 supernovae with 10^{51} erg per million years per ${\rm kpc}^2$ for the solar neighborhood, which yields about $0.7 \times 10^{-4}\,{\rm erg\,cm^{-2}\,s^{-1}}$, i.e., nearly two orders of magnitude more than needed (Brandenburg and Nordlund 2011).

Turbulence with these values of $u_{\rm rms}$ and a correlation length $\ell = 70\,{\rm pc}$ (Shukurov 2005), corresponding to a correlation wavenumber $k_{\rm f} = 2\pi/\ell$ is expected to produce turbulent diffusion with a magnetic diffusion coefficient $\eta_{\rm t} = u_{\rm rms}/3k_{\rm f} \approx 10^{25}\,{\rm cm^2\,s^{-1}} \approx 0.04\ {\rm kpc\,km\,s^{-1}}$, which would lead to turbulent decay of a magnetic field with a vertical wavenumber of $k = 2\pi/0.3\,{\rm kpc} \approx 20\,{\rm kpc^{-2}}$ on a decay time of about $(\eta_{\rm t} k^2)^{-1} \approx 60\,{\rm Myr}$. Thus, to sustain such a field, a dynamo process is required.

Magnetic fields affect the velocity through the Lorentz force. However, if one only wants to understand the origin of the magnetic field, we would be interested in early times when the mean magnetic field is still weak. In that case we can consider the case when the velocity field is still unaffected by the magnetic field and it can thus be considered given. This leads to a kinematic problem that is linear.

Several dynamo processes are known. Of particular relevance are large-scale dynamos that produce magnetic fields on scales large compared with the size of the turbulent eddies. These dynamos are frequently being modeled using mean-field dynamo theory, which means that one solves the averaged induction equation. In such a formulation, the mean electromotive force resulting from correlations of small-scale velocity and magnetic field fluctuations are being parameterized as functions of the mean magnetic field itself, which leads to a closed system of equations. The resulting mean-field equations can have exponentially growing or decaying solutions. Of particular interest is here the question regarding the symmetry properties of the resulting magnetic field. This aspect will be discussed in Sect. 19.2.

Next, the magnetic field will eventually be subject to nonlinear effects and saturate. The most primitive form of nonlinearity is α quenching, which limits the α effect such that the energy density of the local mean magnetic field strength is of the order of the kinetic energy of the turbulence. There is the possibility of so-called catastrophic quenching, which has sometimes been argued to suppress not only turbulent diffusion (Cattaneo and Vainshtein 1991), but also the dynamo effect (Vainshtein and Cattaneo 1992). Those aspects will be discussed in Sect. 19.3. It is now understood that catastrophic quenching is a consequence of magnetic helicity conservation and the fact that the magnetic field takes the form of a bi-helical field with magnetic helicity at different scales and signs. Such a field might have observational signatures that could be observable, as will be discussed in Sect. 19.4.

An entirely different alternative is that a primordial magnetic field might still exist. It would be of interest to find out what effects it would have. This affects the discussion of the initial turbulent magnetic field, which might occur in conjunction with magnetic helicity, which requires some knowledge about turbulent cascades that we shall also discuss in connection with dynamos, so we postpone the discussion of primordial magnetic fields until Sect. 19.5, and begin with kinematic mean-field theory.

19.2 Aspects of Kinematic Mean-Field Theory

The purpose of this section is to review some of the important results in applying mean-field dynamo theory to galaxies. We focus here on linear models and postpone the discussion of essentially nonlinear effects to Sect. 19.3.

19.2.1 Dominance of Quadrupolar Modes

Mean-field dynamo theory for galaxies (Parker 1971; Vainshtein and Ruzmaikin 1971) was developed soon after the corresponding theory for solar, stellar and planetary dynamos was first proposed (Parker 1955; Steenbeck et al. 1966; Steenbeck and Krause 1969a,b). The main difference to stellar dynamos is the flat geometry. An important consequence of this is the finding that the lowest eigenmode is of quadrupolar type, which means that the toroidal magnetic field has the same direction on both sides of the midplane. An example of this is shown in Fig. 19.1, where we show vectors of the magnetic field in the xy plane of the galactic disc together with a xz section approximately through the disc axis. We note that this model has been calculated in Cartesian geometry, which leads to minor artifacts as can be seen in two corners.

The models in galactic geometry made use of the fact that in flat geometries, derivatives in the vertical (z) direction are much more important than in the radial or azimuthal directions. One therefore deals essentially with one-dimensional models of the form (Ruzmaikin et al. 1988),

$$\dot{\overline{B}}_R = -(\alpha \overline{B}_\phi)' + \eta_\mathrm{T} \overline{B}_R'', \quad \dot{\overline{B}}_\phi = S \overline{B}_R + \eta_\mathrm{T} \overline{B}_\phi''. \tag{19.1}$$

Here, primes and dots denote z and t derivatives, respectively, $\alpha = \alpha_0 f_\alpha(z)$ is a profile for α (antisymmetric with respect to $z = 0$) with typical value α_0, $S = R\mathrm{d}\Omega/\mathrm{d}R$ is the radial shear in the disc, and $(\overline{B}_R, \overline{B}_\phi, \overline{B}_z)$ are the components of the mean field $\overline{\boldsymbol{B}}$ in cylindrical coordinates. On $z = \pm H$ one assumes vacuum boundary conditions which, in this one-dimensional problem, reduce to $\overline{B}_R = \overline{B}_\phi = 0$. One can also impose boundary conditions on the mid-plane, $z = 0$, by

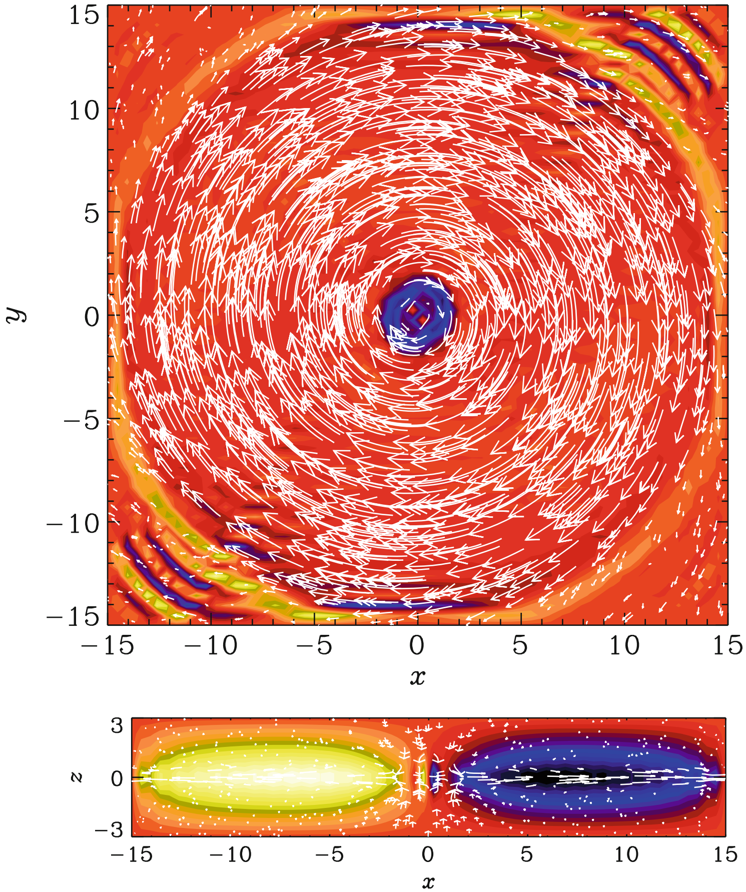

Fig. 19.1 Magnetic field in the midplane of a simplified model of a galaxy with α effect and Brandt rotation curve

selecting either symmetric (quadrupolar) fields, $B_R = \overline{B}'_\phi = 0$, or antisymmetric (dipolar) fields, $B'_R = \overline{B}_\phi = 0$. We define two dimensionless control parameters,

$$C_\Omega = SH^2/\eta_\mathrm{T}, \quad C_\alpha = \alpha_0 H/\eta_\mathrm{T}, \tag{19.2}$$

which measure the strengths of shear and α effects, respectively.

In the limit of strong differential rotation, $C_\alpha/C_\Omega \ll 1$, the solutions are characterized by just one parameter, the dynamo number $D = C_\alpha C_\Omega$. Figure 19.2 shows the growth rate of different modes, obtained by solving Eq. (19.1) for both signs of the dynamo number (Brandenburg 1998). To find all the modes, even the unstable ones, one can solve Eq. (19.1) numerically as an eigenvalue problem, where the complex growth rate λ is the eigenvalue with the largest real part. Note that the

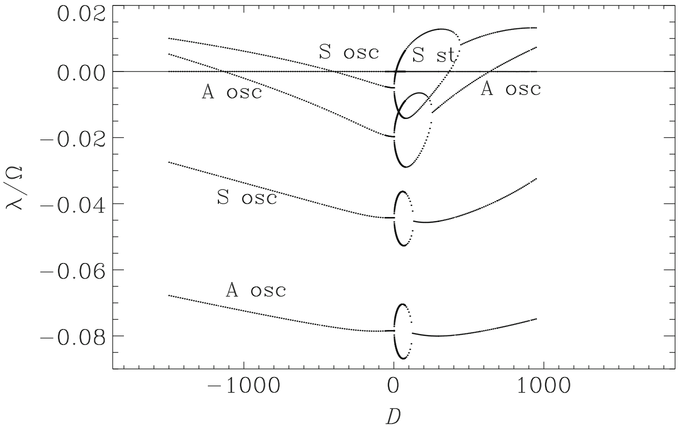

Fig. 19.2 Eigenvalues of the dynamo equations with radial shear in slab geometry. The dynamo number is defined positive when shear is negative and α positive. Note that for $\alpha > 0$, the most easily excited solution is non-oscillatory ('steady') and has even parity (referred to as 'S st') while for $\alpha < 0$ it is oscillatory ('S osc'). Adapted from Brandenburg (1998)

most easily excited mode is quadrupolar and non-oscillatory. We denote it by 'S st', where 'S' refers to symmetry about the midplane and 'st' refers to steady, as opposed to oscillatory. Of course, only in the marginally excited case those modes are really steady.

The basic dominance of quadrupolar magnetic fields is also reproduced by more recent global simulations such as those of Gissinger et al. (2009). However, the situation might be different in so-called cosmic-ray driven dynamos (see below), where the magnetic field could be preferentially dipolar with a reversal of the toroidal field about the midplane (Hanasz et al. 2009). The possibility of a significant dipolar component has also been found for the magnetic field of our Galaxy (Jansson and Farrar 2012). On the other hand, in the inner parts of the galaxy, the geometrical properties of the bulge may also give rise to a locally dipolar field in the center (Donner and Brandenburg 1990).

19.2.2 Non-Axisymmetric Magnetic Fields

An important realization due to Rädler (1986b) was that non-axisymmetric solutions are never favored by differential rotation, because it winds up such fields, so anti-parallel field lines are being brought close together and then decay rapidly, as can be seen from Fig. 19.3. This was already found in earlier numerical eigenvalue calculations (Rädler 1980, 1986a), suggesting that corresponding asymptotic calculations that make the so-called $\alpha\Omega$ approximation (Ruzmaikin et al. 1985), in which the α effect is neglected compared with the shear term, could be problematic.

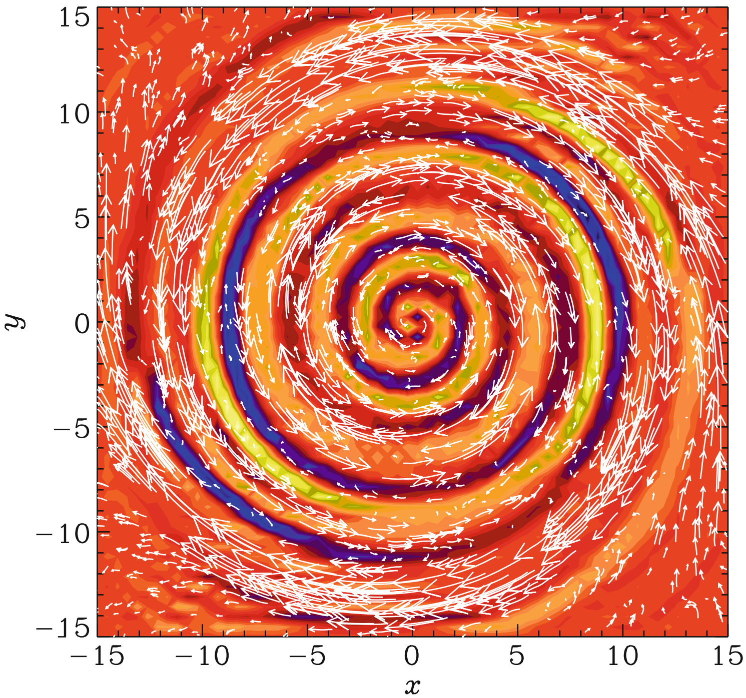

Fig. 19.3 Magnetic field in the midplane of a simplified model of a galaxy with Brandt rotation curve and an initially horizontal magnetic field in the x direction that is then being wound up

At the time it was thought that many external galaxies would harbor non-axisymmetric magnetic fields (Sofue et al. 1986), but this view has now changed with the more careful measurements of the toroidal magnetic fields along an azimuthal ring around various external galaxies. This can be seen from plots of the rotation measure at different positions along such an azimuthal ring. The rotation measure is defined as

$$\mathrm{RM} = \mathrm{d}\chi/\mathrm{d}\lambda^2, \tag{19.3}$$

where λ is the wavelength of the radio emission and χ is the angle of the polarization vector determined from the Stokes parameters Q and U as

$$\chi = \tfrac{1}{2}\mathrm{Arctan}(U, Q), \tag{19.4}$$

where Arctan returns all angles between $-\pi$ and π whose tangent yields U/Q. Figure 19.4 shows theoretical RM dependencies on azimuth around projected rings around dynamo models simulating galactic magnetic fields of types 'S0' (symmetric about midplane with $m = 0$) and 'S1' (also symmetric about midplane, but with $m = 1$, i.e., non-axisymmetric). The result is quite clear. When the magnetic

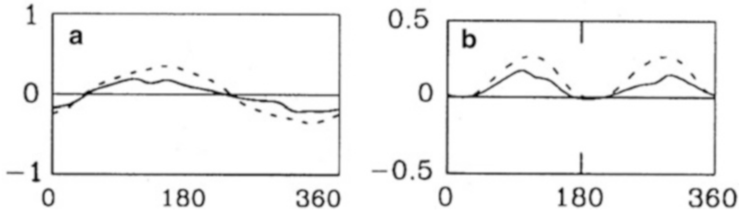

Fig. 19.4 Dependence of RM on the azimuthal angle for (**a**) magnetic field of type S0, and (**b**) magnetic field of type S1. *Solid* and *dashed lines* refer to two different procedures of measuring RM. Adapted from Donner and Brandenburg (1990)

field is axisymmetric, one expects the toroidal magnetic field to give a line-of-sight component $B_{\|}$ and point toward the observer at one azimuthal position on the projected azimuthal ring and away from the observer on the opposite position along the ring. This should lead to a sinusoidal modulation of RM with one positive extremum and one negative one. When the field is bisymmetric (i.e., non-axisymmetric with $m = 1$), one expects two positive extrema and two negative ones. This is indeed borne out by the simulations. It is this type of evidence that led to the conclusion that the magnetic field of M81 is non-axisymmetric (Krause et al. 1989).

Even today, M81 is still the one and only example of a galaxy displaying a distinctly non-axisymmetric magnetic field with azimuthal order $m = 1$ (Beck et al. 1996); see also the Chapter by Beck in this volume on observations of galactic magnetic fields. Such fields are hard to explain theoretically, because, according to most of the dynamo models presented so far, non-axisymmetric modes are always harder to excite than axisymmetric ones; see also Brandenburg et al. (1989) for a survey of such solutions. The currently perhaps best explanation for non-axisymmetric magnetic fields in galaxies is that they are a left-overs from the initial conditions and are being wound up by the differential rotation. This can be a viable explanation only because for galaxies the turbulent decay time might be slow enough, especially in their outer parts, if those fields are helical and non-kinematic (Blackman and Subramanian 2013; Bhat et al. 2014). Moss et al. (1993) presented a model that incorporated a realistic representation of the so-called peculiar motions of M81 that were proposed to be the result of a recent close encounter with a companion galaxy. These peculiar motions are flows relative to the systematic differential rotation and have been obtained from an earlier stellar dynamics simulation by Thomasson and Donner (1993). A very different alternative is that the $m = 1$ magnetic fields in the outskirts of M81 are driven by the magneto-rotational instability, as has recently been proposed by Gressel et al. (2013).

A more typical class of non-axisymmetric fields are those with $m = 2$ and $m = 0$ contributions. Those would no longer be called bisymmetric and fall outside the old classification into axisymmetric and bisymmetric spirals. Examples of non-axisymmetric but non-bisymmetric spirals are NGC 6946 and IC 342 (e.g. Beck 2007; Beck and Wielebinski 2013). A natural way of explaining such fields is via non-axisymmetric dynamo parameters such as the α-effect (Mestel and

Subramanian 1991; Moss et al. 1991; Subramanian and Mestel 1993). This has been confirmed through more realistic modeling both with (Chamandy et al. 2013, 2014) and without (Moss et al. 2013) memory effect. For a more popular account on recent modeling efforts, see also the review by Moss (2012).

19.2.3 The α Effect and Turbulent Diffusivity in Galaxies

The forcing of turbulence through the pressure force associated with the thermal expansion of blast waves is essentially irrotational. However, vorticity is essential for what is known as small-scale dynamo action, and it is also a defining element of kinetic helicity and hence the α effect, which is an important parameter in mean-field simulations of galactic dynamos. In galaxies, the baroclinic term is an important agent for making the resulting flow vortical (Korpi et al. 1998); see also Del Sordo and Brandenburg (2011), who compared with the effects of rotation and shear. Thus, we need to know how efficiently vorticity can be generated in turbulence. This question becomes particularly striking in the case of isothermal turbulence, because then, and in the absence of rotation, shear, or magnetic fields, there is no baroclinic term that could generate vorticity. In that case, vorticity can only be generated via viscosity through a "visco-clinic" term of the form $\nabla \ln \rho \times \nabla \mathrm{div}\, \boldsymbol{u}$, although it is not obvious that this term is unaffected by the numerical form of the diffusion operator.

Most of the papers assume that it is a result of cyclonic turbulent motions driven by supernova explosions. There have also been attempts to calculate α and η_{t} by considering individual explosions (Ferrière 1992) and also so-called superbubbles resulting from several explosions that could have triggered each other (Ferrière 1993).

Nowadays, a reliable method for calculating α and η_{t} from numerical simulations is the test-field method, which will be briefly discussed below. The α effect and turbulent diffusivity η_{t} characterize the resulting electromotive force $\overline{\boldsymbol{\mathcal{E}}}$ from small-scale (unresolved) motions, i.e., $\overline{\boldsymbol{\mathcal{E}}} = \overline{\boldsymbol{u} \times \boldsymbol{b}}$. This expression enters in the evolution equation for the mean magnetic field,

$$\frac{\partial \overline{\boldsymbol{B}}}{\partial t} = \nabla \times \left(\overline{\boldsymbol{U}} \times \overline{\boldsymbol{B}} + \overline{\boldsymbol{u} \times \boldsymbol{b}} - \eta \mu_0 \overline{\boldsymbol{J}} \right). \tag{19.5}$$

To determine $\overline{\boldsymbol{u} \times \boldsymbol{b}}$ as a function of $\overline{\boldsymbol{B}}$, which drives magnetic fluctuations $\boldsymbol{b} = \boldsymbol{B} - \overline{\boldsymbol{B}}$ through tangling by the turbulent motions $\boldsymbol{U} = \overline{\boldsymbol{U}} + \boldsymbol{u}$, we use the evolution equation for $\boldsymbol{b}$ obtained by subtracting Eq. (19.5) from the full induction equation

$$\frac{\partial \boldsymbol{B}}{\partial t} = \nabla \times (\boldsymbol{U} \times \boldsymbol{B} - \eta \mu_0 \boldsymbol{J}), \tag{19.6}$$

with the result

$$\frac{\partial \boldsymbol{b}}{\partial t} = \nabla \times \left(\overline{\boldsymbol{U}} \times \boldsymbol{b} + \boldsymbol{u} \times \overline{\boldsymbol{B}} + \boldsymbol{u} \times \boldsymbol{b} - \overline{\boldsymbol{u} \times \boldsymbol{b}} - \eta_{\rm t}\mu_0 \boldsymbol{j} \right), \tag{19.7}$$

where $\boldsymbol{J} = \overline{\boldsymbol{J}} + \boldsymbol{j}$ is the current density decomposed into mean and fluctuating parts, μ_0 is the vacuum permeability, and η is the Spitzer value of the magnetic diffusivity. We solve Eq. (19.7) for mean fields $\overline{\boldsymbol{B}}$ that do not need to be a solution of Eq. (19.5); see Schrinner et al. (2005, 2007). We can then compute $\overline{\boldsymbol{u} \times \boldsymbol{b}}$, related it to the chosen test fields and their derivatives, $\overline{B}_i$ and $\partial \overline{B}_i / \partial x_j$, and determine all relevant components of α_{ij} and η_{ijk}, which requires a corresponding number of test fields.

There is by now a lot of literature on this topic. The method has been extended into the quasi-kinematic (Brandenburg et al. 2008a) and fully nonlinear (Rheinhardt and Brandenburg 2010) regimes. For moderate scale separation, a convolution in space and time can often not be ignored (Brandenburg et al. 2008b; Hubbard and Brandenburg 2009), but it is possible to incorporate such effects in an approximate fashion by solving an evolution equation for the mean electromotive force (Rheinhardt and Brandenburg 2012). Such an approach restores causality in the sense that the elliptic nature of the diffusion equation takes the form of a wave equation, which limits effectively the maximum propagation speed to the rms velocity of the turbulence (Brandenburg et al. 2004). Such an equation is usually referred to as the telegraph equation. In galaxies, such an effect can also cause magnetic arm to lag the corresponding material arm with respect to the rotation (Chamandy et al. 2013).

Gressel et al. (2008b) have applied the test-field method to their turbulent galactic dynamo simulations (Gressel et al. 2008a) and find values for $\eta_{\rm t}$ that are of the order of 1 kpc km s^{-1} (see Fig. 19.5), which corresponds to 3×10^{26} cm^2 s^{-1}, which is 30 times larger than our naive estimate presented in the introduction. In their simulations, $u_{\rm rms} \approx 40$ km/s, so their effective value of $k_{\rm f}$ must be $k_{\rm f} \approx u_{\rm rms}/3\eta_{\rm t} \approx 13$ kpc^{-1}, and their effective correlation length thus $2\pi/k_{\rm f} \approx 0.5$ kpc, instead of our

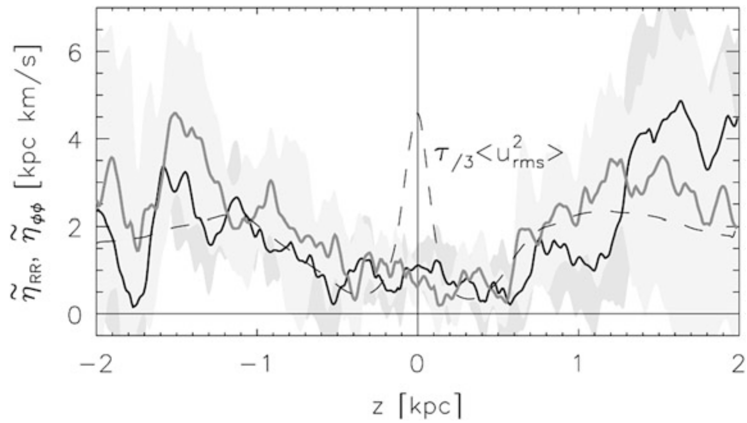

Fig. 19.5 Vertical dependence of $\eta_{\rm t}$ obtained by the test-field method using a simulation of supernova-driven turbulence. Adapted from Gressel et al. (2008b)

estimate of only 0.07 kpc. The reason for this discrepancy in unclear and highlights the importance of doing numerical simulations. Their values for α are positive in the upper disc plane and increase approximately linearly to about $5\,\mathrm{km\,s^{-1}}$ at a height of 1 kpc. This allows us to estimate the fractional helicity as $\varepsilon_\mathrm{f} \approx \alpha/\eta_\mathrm{t} k_\mathrm{f} \approx 0.1$ (cf. Blackman and Brandenburg 2002).

An additional driver of the α effect is the possibility of inflating magnetic flux tubes by cosmic rays (Parker 1992). This makes such magnetic flux tubes buoyant and, together with the effects of rotation and stratification, leads to an α effect. This has led to successful simulations of galactic dynamos both in local (Hanasz et al. 2004) and global (Hanasz et al. 2009; Kulpa-Dybeł et al. 2011) geometries. Cosmic rays are usually treated in the diffusion approximation with a diffusion tensor proportional to $B_i B_j$ that forces the diffusion to be only along magnetic field lines. However, the effective diffusivity is very large (in excess of $10^{28}\,\mathrm{cm^2\,s^{-1}}$), making an explicit treatment costly because of a short diffusive time step constraint. Again, one can make use of the telegraph equation to limit the diffusion speed to a speed not much faster than the speed of sound. Such an approach has been exploited by Snodin et al. (2006), but it has not yet been applied to more realistic cosmic ray-driven dynamos.

19.3 Aspects of Nonlinear Mean-Field Theory

19.3.1 Bi-Helical Magnetic Fields from Simulations

When the computational domain is large enough and turbulence is driven in a helical fashion at a small length scale, one sees the clear emergence of what is called a bi-helical magnetic field. An example is shown in Fig. 19.6 where we show magnetic

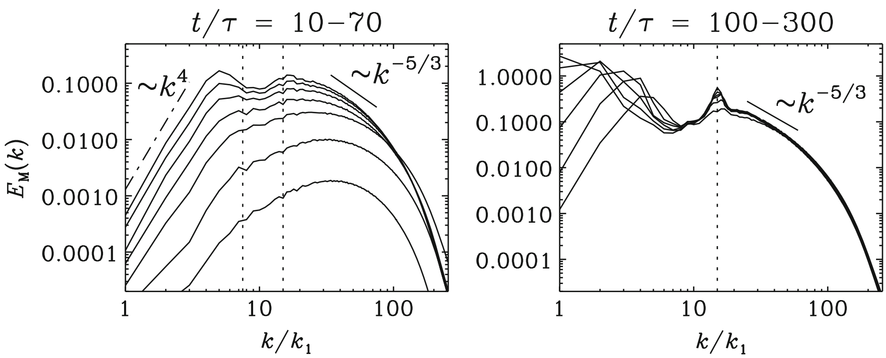

Fig. 19.6 Magnetic energy spectra $E_\mathrm{M}(k)$, at earlier (*left*) and later (*right*) times. The scale separation ratio is $k_\mathrm{f}/k_1 = 15$. The range of time t is given in units of the turnover time, $\tau = 1/u_\mathrm{rms}k_\mathrm{f}$. At small wavenumbers, the $E_\mathrm{M}(k)$ spectrum is proportional to k^4, while to the right of $k_\mathrm{f}/k_1 = 15$ there is a short range with a $k^{-5/3}$ spectrum. Adapted from Brandenburg (2011)

power spectra of a simulation of Brandenburg (2011). During the early evolution of the dynamo (left) we see the growth of the magnetic field at small wavenumbers, accompanied by a growth at small amplitude at lower wavenumbers. The spectrum remains however roughly shape-invariant.

By $t/\tau > 100$, where τ is the turnover time of the turbulence at the forcing scale, a large-scale field is already present. As the field saturates, the peak of magnetic energy moves to progressively smaller wavenumbers. The reason for this peak can be understood in terms of an α^2 dynamo.

19.3.2 Catastrophic Quenching

The idea of catastrophic quenching is almost as old as mean-field dynamo theory itself. Here, "catastrophic" refers to a (declining) dependence of the turbulent transport coefficients on the magnetic Reynolds number, Re_M, even when Re_M is already very large. The word 'catastrophic' was first used by Blackman and Field (2000) to indicate the fact that in the astrophysical context, the α effect would become catastrophically small. The issue focussed initially on turbulent diffusion (Knobloch 1978; Layzer et al. 1979; Piddington 1981). Numerical simulations later showed that in two dimensions, with a large-scale magnetic field lying in that plane, the decay of this large-scale field is indeed slowed down in an Re_M-dependent (i.e., catastrophic) fashion (Cattaneo and Vainshtein 1991). This then translates into a corresponding Re_M-dependent quenching of the effective turbulent magnetic diffusivity. Later, Vainshtein and Cattaneo (1992) argued that also the α effect would be catastrophically quenched, possibly with an even higher power of Re_M.

Gruzinov and Diamond (1994) later realized that the Re_M dependence is associated with the presence of certain conservation laws which are different in two and three dimensions. In three dimensions, the magnetic helicity, $\langle \boldsymbol{A} \cdot \boldsymbol{B} \rangle$, is conserved, while in two dimensions, $\langle A^2 \rangle$ is conserved. Here and elsewhere, angle brackets denote averaging, and A is the component of $\boldsymbol{A}$ that is perpendicular to the plane in two dimensions.

In three dimensions, the suppression of the large-scale dynamo effect can be understood by considering the fact that the field generated by an α-effect dynamo is helical and of Beltrami type, e.g., $\overline{\boldsymbol{B}} = (\sin k_1 z, \cos k_1 z, 0) B_0$, which is parallel to its curl, i.e., $\nabla \times \overline{\boldsymbol{B}} = (\sin k_1 z, \cos k_1 z, 0) k B_0 = k_1 \overline{\boldsymbol{B}}$. The vector potential can then be written as $\overline{\boldsymbol{A}} = k_1^{-1} \overline{\boldsymbol{B}}$, so that the magnetic helicity is $\langle \overline{\boldsymbol{A}} \cdot \overline{\boldsymbol{B}} \rangle = k_1^{-1} B_0^2$. The current helicity is $\langle \overline{\boldsymbol{J}} \cdot \overline{\boldsymbol{B}} \rangle = k_1 B_0^2 / \mu_0$. Note, however, that magnetic helicity of the total field is conserved. Since the total field is given by the sum of large and small-scale components, $\boldsymbol{B} = \overline{\boldsymbol{B}} + \boldsymbol{b}$, the generation of magnetic helicity at large scales can be understood if there is a corresponding production of magnetic helicity at small scales, but of opposite sign. The magnetic and current helicities of the small-scale field can be estimated analogously as $\langle \boldsymbol{a} \cdot \boldsymbol{b} \rangle = -k_\mathrm{f}^{-1} \langle \boldsymbol{b}^2 \rangle$ and $\langle \boldsymbol{j} \cdot \boldsymbol{b} \rangle = -k_\mathrm{f} \langle \boldsymbol{b}^2 \rangle / \mu_0$, respectively.

The relative importance of large-scale and small-scale contributions to magnetic helicity and magnetic energy is determined by the magnetic helicity equation,

$$\frac{\mathrm{d}}{\mathrm{d}t}\langle \boldsymbol{A}\cdot\boldsymbol{B}\rangle = -2\eta\mu_0\langle \boldsymbol{J}\cdot\boldsymbol{B}\rangle. \tag{19.8}$$

Inserting $\langle \boldsymbol{A}\cdot\boldsymbol{B}\rangle = \langle \overline{\boldsymbol{A}}\cdot\overline{\boldsymbol{B}}\rangle + \langle \boldsymbol{a}\cdot\boldsymbol{b}\rangle$ and $\langle \boldsymbol{J}\cdot\boldsymbol{B}\rangle = \langle \overline{\boldsymbol{J}}\cdot\overline{\boldsymbol{B}}\rangle + \langle \boldsymbol{j}\cdot\boldsymbol{b}\rangle$, and applying it to the time after which the small-scale field has already reached saturation, i.e., $\langle \boldsymbol{b}^2\rangle = \text{const}$, we have

$$k_1^{-1}\frac{\mathrm{d}}{\mathrm{d}t}\langle \overline{\boldsymbol{B}}^2\rangle = -2\eta k_1\langle \overline{\boldsymbol{B}}^2\rangle + 2\eta k_\mathrm{f}\langle \boldsymbol{b}^2\rangle. \tag{19.9}$$

One sees immediately that the steady state solution is $\langle \overline{\boldsymbol{B}}^2\rangle/\langle \boldsymbol{b}^2\rangle = k_\mathrm{f}/k_1 > 1$, i.e., the large-scale field exceeds the small-scale field by a factor that is equal to the scale separation ratio. Moreover, this steady state is only reached on a resistive time scale. Since $\langle \boldsymbol{b}^2\rangle$ is assumed constant in time, we can integrate Eq. (19.9) to give

$$\langle \overline{\boldsymbol{B}}^2\rangle = \langle \boldsymbol{b}^2\rangle \frac{k_\mathrm{f}}{k_1}\left[1 - e^{-2\eta k_1^2 (t - t_\mathrm{sat})}\right], \tag{19.10}$$

which shows that the relevant resistive time scale is $(2\eta k_1^2)^{-1}$. This saturation behavior agrees well with results from simulations; see Fig. 19.7.

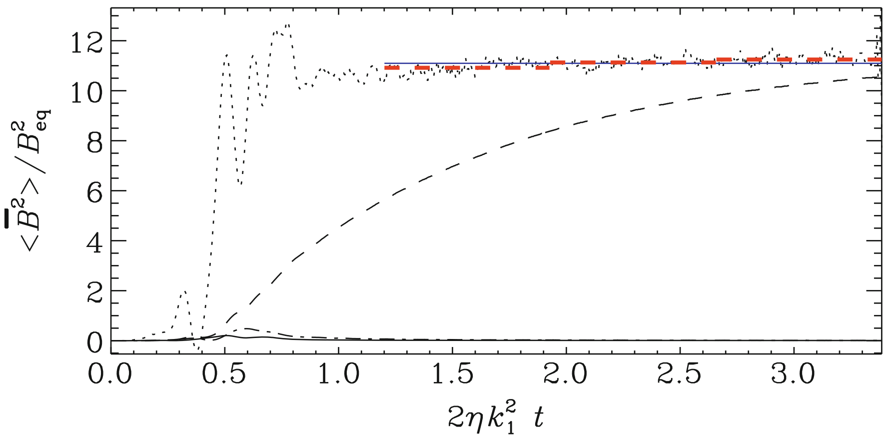

Fig. 19.7 Example showing the evolution of the normalized $\langle \overline{\boldsymbol{B}}^2\rangle$ (*dashed*) and that of $\langle \overline{\boldsymbol{B}}^2\rangle + \mathrm{d}\langle \overline{\boldsymbol{B}}^2\rangle/\mathrm{d}(2\eta k^2 t)$ (*dotted*), compared with its average in the interval $1.2 \le 2\eta k_1^2 t \le 3.5$ (*horizontal blue solid line*), as well as averages over three subintervals (*horizontal red dashed lines*). Here, $\overline{\boldsymbol{B}}$ is evaluated as an xz average, $\langle \boldsymbol{B}\rangle_{xz}$. For comparison we also show the other two averages, $\langle \boldsymbol{B}\rangle_{xy}$ (*solid*) and $\langle \boldsymbol{B}\rangle_{yz}$ (*dash-dotted*), but their values are very small. Adapted from Candelaresi and Brandenburg (2013)

19.3.3 Mean-Field Description

The simplistic explanation given above can be reproduced in mean-field dynamo theory when magnetic helicity conservation is introduced as an extra constraint. Physically, such a constraint is well motivated and goes back early work of Pouquet et al. (1976), who found that the relevant α in the mean-field dynamo is given by the sum of kinetic and magnetic contributions,

$$\alpha = \alpha_\mathrm{K} + \alpha_\mathrm{M}, \tag{19.11}$$

where $\alpha_\mathrm{K} = -(\tau/3)\langle\boldsymbol{\omega}\cdot\boldsymbol{u}\rangle$ is the formula for the kinematic value in the high conductivity limit (Moffatt 1978; Krause and Rädler 1980), and $\alpha_\mathrm{M} = (\tau/3\overline{\rho})\langle\boldsymbol{j}\cdot\boldsymbol{b}\rangle$ is the magnetic contribution. Again, under isotropic conditions, $\langle\boldsymbol{j}\cdot\boldsymbol{b}\rangle$ is proportional to $\langle\boldsymbol{a}\cdot\boldsymbol{b}\rangle$, with the coefficient of proportionality being k_f^2. This is because the spectra of magnetic and current helicity, $H(k)$ and $C(k)$, which are normalized such that $\int H(k)\,\mathrm{d}k = \langle\boldsymbol{A}\cdot\boldsymbol{B}\rangle$ and $\int C(k)\,\mathrm{d}k = \langle\boldsymbol{J}\cdot\boldsymbol{B}\rangle$, are proportional to each other with $C(k) = k^2 H(k)$, so the proportionality between small-scale current and magnetic helicities is obtained by applying $C(k) = k^2 H(k)$ to $k = k_\mathrm{f}$. Even in an inhomogeneous system, this approximation is qualitatively valid, except that the coefficient of proportionality is found to be somewhat larger (Mitra et al. 2010; Hubbard and Brandenburg 2010; Del Sordo et al. 2013).

The question is now how to obtain $\langle\boldsymbol{a}\cdot\boldsymbol{b}\rangle$. One approach is to evolve $\overline{\boldsymbol{A}}$ (instead of $\overline{\boldsymbol{B}}$) in a mean-field model and compute at each time step (Hubbard and Brandenburg 2012) $\langle\boldsymbol{a}\cdot\boldsymbol{b}\rangle = \langle\boldsymbol{A}\cdot\boldsymbol{B}\rangle - \langle\overline{\boldsymbol{A}}\cdot\overline{\boldsymbol{B}}\rangle$, where $\langle\boldsymbol{A}\cdot\boldsymbol{B}\rangle$ obeys Eq. (19.8) for the total magnetic helicity. In practice, one makes an important generalization in that volume averaging is relaxed to mean just averaging over one or at most two coordinate directions. (To obey Reynolds rules, these coordinate directions should be periodic.) Thus, Eq. (19.8) then becomes

$$\frac{\partial}{\partial t}\overline{\boldsymbol{A}\cdot\boldsymbol{B}} = -2\eta\mu_0\overline{\boldsymbol{J}\cdot\boldsymbol{B}} - \nabla\cdot\overline{\mathscr{F}}, \tag{19.12}$$

where $\overline{\mathscr{F}}$ is the magnetic helicity flux from both large-scale and small-scale fields. Hubbard and Brandenburg (2012) pointed out that this approach can be superior to the traditional approach by Kleeorin and Ruzmaikin (1982), in which one solves instead the evolution equation for $\langle\boldsymbol{a}\cdot\boldsymbol{b}\rangle$,

$$\frac{\partial}{\partial t}\overline{\boldsymbol{a}\cdot\boldsymbol{b}} = -2\overline{\mathscr{E}}\cdot\overline{\boldsymbol{B}} - 2\eta\mu_0\overline{\boldsymbol{j}\cdot\boldsymbol{b}} - \nabla\cdot\overline{\mathscr{F}}_\mathrm{f}, \tag{19.13}$$

where $\overline{\mathscr{F}}_\mathrm{f}$ is the magnetic helicity flux only from the small-scale magnetic field. The two approaches are equivalent, except that there is an ambiguity as to what should be included in $\overline{\mathscr{F}}_\mathrm{f}$. In particular, when deriving the evolution equation for $\langle\overline{\boldsymbol{A}}\cdot\overline{\boldsymbol{B}}\rangle$ in the Weyl gauge, i.e., using just $\partial\overline{\boldsymbol{A}}/\partial t = \overline{\mathscr{E}} - \eta\mu_0\overline{\boldsymbol{J}}$, we obtain

$$\frac{\partial}{\partial t}(\overline{\boldsymbol{A}} \cdot \overline{\boldsymbol{B}}) = 2\overline{\mathcal{E}} \cdot \overline{\boldsymbol{B}} - 2\eta\mu_0 \overline{\boldsymbol{J}} \cdot \overline{\boldsymbol{B}} - \nabla \cdot (-\overline{\mathcal{E}} \times \overline{\boldsymbol{A}}), \tag{19.14}$$

i.e., there is an extra flux term $-\overline{\mathcal{E}} \times \overline{\boldsymbol{A}}$. Thus, as argued by Hubbard and Brandenburg (2012), if $\overline{\mathcal{F}} = \overline{\mathcal{F}}_{\rm m} + \overline{\mathcal{F}}_{\rm f} = \boldsymbol{0}$, this implies that $\overline{\mathcal{F}}_{\rm f} = \overline{\mathcal{E}} \times \overline{\boldsymbol{A}}$ in Eq. (19.14).

19.3.3.1 Diffusive Magnetic Helicity Fluxes and Gauge Issues

Another important contribution to the magnetic helicity flux is a turbulent-diffusive flux down the gradient of magnetic helicity density. In Fig. 19.8 we show the profiles of $\langle \overline{\mathcal{E}} \cdot \overline{\boldsymbol{B}} \rangle$ and $\eta \langle \overline{\boldsymbol{J}} \cdot \overline{\boldsymbol{B}} \rangle$ from a simulation of Hubbard and Brandenburg (2010), compare the residual $2\langle \overline{\mathcal{E}} \cdot \overline{\boldsymbol{B}} \rangle - 2\eta \langle \overline{\boldsymbol{J}} \cdot \overline{\boldsymbol{B}} \rangle$ with the divergence of the magnetic helicity flux, and finally compare the flux $\overline{\mathcal{F}}_{\rm f} = \overline{\boldsymbol{e} \times \boldsymbol{a}}$ with that obtained from the diffusion approximation, $-\kappa_{\rm f} \boldsymbol{\nabla} \overline{h}_{\rm f}$. These results demonstrate that there is indeed a measurable difference between $\langle \overline{\mathcal{E}} \cdot \overline{\boldsymbol{B}} \rangle$ and $\eta \langle \overline{\boldsymbol{J}} \cdot \overline{\boldsymbol{B}} \rangle$, which can be explained by a magnetic helicity flux divergence, and that this magnetic helicity flux can be understood as a turbulent-diffusive one, i.e., down the gradient of the local magnetic helicity density.

At this point, a comment about gauge-dependencies is in order. First of all, in the framework of large-scale dynamos, one expects scale separation between small-scale and large-scale magnetic fields. It is then possible to express the small-scale magnetic helicity as a density of linkages between magnetic structures, which leads to the manifestly gauge-invariant Gauss linking formula (Subramanian and Brandenburg 2006). Second, the large-scale magnetic field remains in general gauge-dependent, and there have been several examples of this (Brandenburg et al. 2002; Hubbard and Brandenburg 2010). This would render the alternate approach

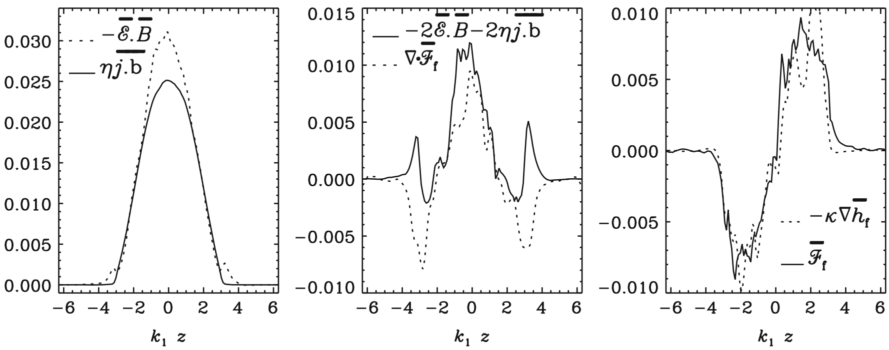

Fig. 19.8 Time-averaged terms on the right-hand side of (19.13), $\langle \overline{\mathcal{E}} \cdot \overline{\boldsymbol{B}} \rangle_T$ and $\eta \langle \boldsymbol{j} \cdot \boldsymbol{b} \rangle_T$ (*left panel*), the difference between these terms compared with the magnetic helicity flux divergence of small-scale fields $\langle \boldsymbol{\nabla} \cdot \overline{\mathcal{F}}_{\rm f}^{\rm W} \rangle_T$ (*middle panel*), and the flux itself compared with the Fickian diffusion ansatz (*right-hand panel*). Adapted from Hubbard and Brandenburg (2010)

of Hubbard and Brandenburg (2012) problematic, but they argue that those gauge-dependencies result simply from a drift in the mean vector potential and must be subtracted out. Third, with appropriate boundary conditions, such drifts can be eliminated, and $\langle \boldsymbol{A} \cdot \boldsymbol{B} \rangle$ can then well reach a statistically steady state. If that is the case, the left-hand side of Eq. (19.12) vanishes after time averaging, so the gauge-dependent magnetic helicity flux divergence must balance the gauge-independent resistive term, so the former must in fact also be gauge-independent (Mitra et al. 2010; Hubbard and Brandenburg 2010). This argument applies even separately to the contributions from small-scale and large-scale components; see Eqs. (19.13) and (19.14). This allowed Del Sordo et al. (2013) to show for the first time that the magnetic helicity flux divergence from the small-scale field can become comparable to the resistive term. Ultimately, however, one expects it of course to out-compete the latter, but this has not yet been seen for the magnetic Reynolds numbers accessible to date.

The issue of magnetic helicity fluxes occurs already in the special case of a closed domain for which $\langle \nabla \cdot \overline{\mathscr{F}} \rangle = 0$, i.e., $\oint \overline{\mathscr{F}} \cdot \mathrm{d}\boldsymbol{S} = 0$, so there is no flux in or out of the domain, but $\overline{\mathscr{F}}$ and $\overline{\mathscr{F}}_{\mathrm{f}}$ can still be non-vanishing within the domain. This is the case especially for shear flows, where the flux term can have a component in the cross-stream direction that is non-uniform and can thus contribute to a finite divergence. Simulations of Hubbard and Brandenburg (2012) have shown that such a term might be an artifact of choosing the Coulomb gauge rather than the so-called advective gauge, in which case such a term would vanish. This implies that the shear-driven Vishniac and Cho (2001) flux would vanish. This term was previously thought to be chiefly responsible for alleviating catastrophic quenching in shear flows (Subramanian and Brandenburg 2004; Brandenburg and Sandin 2004). It is therefore surprising that such a simple term is now removed by a simple gauge transformation. Clearly, more work is needed to clarify this issue further.

19.3.3.2 Diffusive Versus Advective Magnetic Helicity Fluxes

To date we know of at least two types of magnetic helicity flux that can alleviate catastrophic quenching. One is a diffusive magnetic helicity fluxes proportional to the negative gradient of the local value of the mean magnetic helicity density from the small-scale fields, $\overline{h}_{\mathrm{f}} = \langle \boldsymbol{a} \cdot \boldsymbol{b} \rangle$, so $\overline{\mathscr{F}}_{\mathrm{f}}^{\mathrm{diff}} = -\kappa_{\mathrm{h}} \nabla \overline{h}_{\mathrm{f}}$. Another is a contribution that comes simply from advection by the mean flow $\overline{\boldsymbol{U}}$, so $\overline{\mathscr{F}}_{\mathrm{f}}^{\mathrm{adv}} = \overline{h}_{\mathrm{f}} \overline{\boldsymbol{U}}$ (Shukurov et al. 2006; Sur et al. 2007). Recent work Mitra et al. (2010) has analyzed the contributions to the evolution equation for $\overline{h}_{\mathrm{f}}$; see Eq. (19.13). In the low Re_M regime, the production term $2\overline{\boldsymbol{\mathscr{E}}} \cdot \overline{\boldsymbol{B}}$ is balanced essentially by $2\eta\mu_0 \overline{\boldsymbol{j} \cdot \boldsymbol{b}}$. This means that, as η decreases, $2\overline{\boldsymbol{\mathscr{E}}} \cdot \overline{\boldsymbol{B}}$ must also decrease, which leads to catastrophic quenching in that regime. However, although the $\nabla \cdot \overline{\mathscr{F}}_{\mathrm{f}}$ term is subdominant, it shows a less steep Re_M-dependence ($\propto \mathrm{Re}_M^{-1/2}$, as opposed to Re_M^{-1} for the $2\eta\mu_0 \overline{\boldsymbol{j} \cdot \boldsymbol{b}}$ term), and has therefore the potential of catching up with the other terms to balance $2\overline{\boldsymbol{\mathscr{E}}} \cdot \overline{\boldsymbol{B}}$ with a less steep scaling.

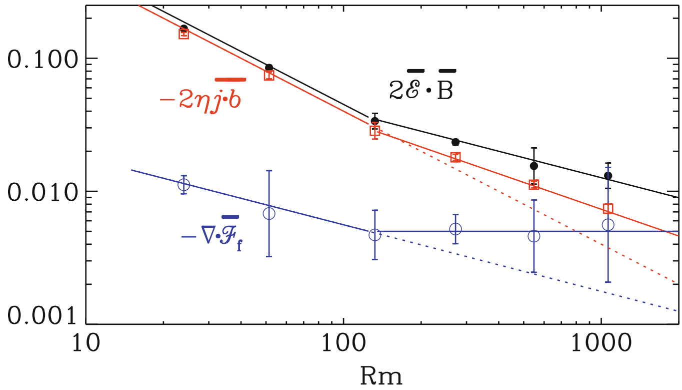

Fig. 19.9 Scaling properties of the vertical slopes of $2\overline{\mathcal{E}}\cdot\overline{\boldsymbol{B}}$, $-2\eta\mu_0\,\overline{\boldsymbol{j}\cdot\boldsymbol{b}}$, and $-\boldsymbol{\nabla}\cdot\overline{\mathcal{F}}_{\rm f}$ for models with a wind. (Given that the three quantities vary approximately linearly with z, the three labels indicate their non-dimensional values at $k_1z = 1$.) The second panel shows that a stronger wind decreases the value of Re_M for which the contribution of the advective term becomes comparable to that of the resistive term. Adapted from Del Sordo et al. (2013)

Recent work using a simple model with a galactic wind has shown, for the first time, that this may indeed be possible. In Fig. 19.9 we show their basic result. As it turns out, below $\mathrm{Re}_M = 100$ the $2\eta\mu_0\overline{\boldsymbol{j}\cdot\boldsymbol{b}}$ term dominates over $\boldsymbol{\nabla}\cdot\overline{\mathcal{F}}$, but because of the different scalings (slopes being -1 and $-1/2$, respectively), the $\boldsymbol{\nabla}\cdot\overline{\mathcal{F}}$ term is expected to become dominant for larger values of Re_M (about 3000). Surprisingly, however, $\boldsymbol{\nabla}\cdot\overline{\mathcal{F}}$ becomes approximately constant for $\mathrm{Re}_M \gtrsim 100$ and $2\eta\mu_0\overline{\boldsymbol{j}\cdot\boldsymbol{b}}$ shows now a shallower scaling (slope $-1/2$). This means that the two curves would still cross at a similar value. Our data suggest, however, that $\boldsymbol{\nabla}\cdot\overline{\mathcal{F}}$ may even rise slightly, so the crossing point is now closer to $\mathrm{Re}_M = 1000$.

19.3.3.3 Magnetic Helicity Fluxes in the Exterior

Some surprising behavior has been noticed in connection with the small-scale magnetic helicity flux in the solar wind, and it is to be expected that such behavior also applies to galaxies. Naively, if negative magnetic helicity from small-scale fields is ejected from the northern hemisphere, one would expect to find negative magnetic helicity at small scales anywhere in the exterior. However, if a significant part of this flux is caused by a diffusive magnetic helicity flux, this expectation might be wrong and the sign changes such that the small-scale magnetic helicity becomes positive some distance away from the dynamo regime. In Fig. 19.10 we reproduce in graphical form the explanation offered by Warnecke et al. (2012).

The idea is that the helicity flux is essentially diffusive in nature. Thus, to transport positive helicity outward, we need a negative gradient, and to transport negative helicity outward, as in the present case, we need a positive gradient outward. This is indeed what is shown in Fig. 19.10. It is then conceivable that the

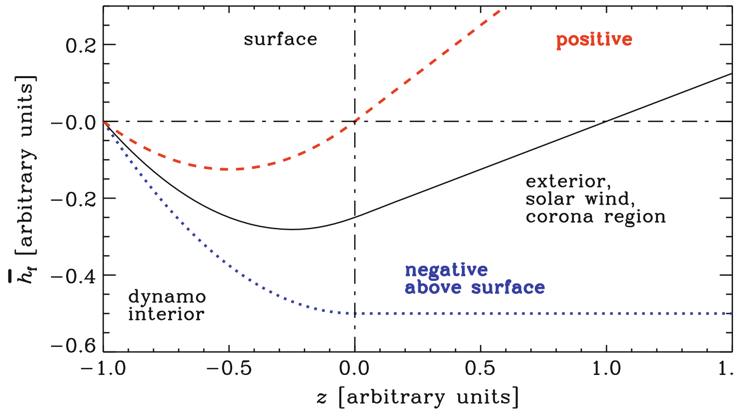

Fig. 19.10 Sketch showing possible solutions $\overline{h}_\mathrm{f}(z)$ with $S = \text{const} = -1$ in $z < 0$ and $S = 0$ in $z > 0$. The *red* (*dashed*) and *black* (*solid*) *lines* show solutions for which the magnetic helicity flux $(-\kappa_h \mathrm{d}\overline{h}_\mathrm{f}/\mathrm{d}z)$ is negative in the exterior. The *blue* (*dotted*) *line* shows the case, where the magnetic helicity flux is zero above the surface and therefore do not reverse the sign of $\overline{h}_\mathrm{f}(z)$ in the exterior. Adapted from Warnecke et al. (2012)

magnetic helicity overshoots and becomes itself positive, which is indeed what is seen in the solar wind (Brandenburg et al. 2011).

19.4 Observational Aspects

It would be an important confirmation of the nonlinear quenching theory if one could find observational evidence for bi-helical magnetic fields. This has not yet been possible, but new generations of radio telescopes allow for a huge coverage of radio wavelengths λ, which could help us determine the spatial distribution of the magnetic field using a tool nowadays referred to as RM synthesis (Brentjens and de Bruyn 2005; Heald et al. 2009; Frick et al. 2011; Gießübel et al. 2013). This refers to the fact that the line-of-sight integral for the complex polarized intensity $P = Q + \mathrm{i}U$ can be written as an integral over the Faraday depth ϕ (which itself is an integral over $B_\parallel$ and, under idealizing assumptions, proportional to the line of sight coordinate z) and takes the form

$$P(\lambda^2) = \int_{-\infty}^{\infty} F(\phi) e^{2\mathrm{i}\phi\lambda^2}\, \mathrm{d}\phi, \tag{19.15}$$

which can be thought of as a Fourier integral for the Fourier variable $2\lambda^2$ (Burn 1966). The function $F(\phi)$ is referred to as the Faraday dispersion function, and it would be interesting to find it by observing $P(\lambda^2)$. The problem is of course that only positive values of λ^2 can be observed.

Most of the work in this field assumes that $P(\lambda^2)$ is Hermitian, i.e., $P(-\lambda^2) = P(\lambda^2)^*$, where the asterisk denotes complex conjugation. This is however not the case for a helical magnetic field, as has recently been pointed out (Brandenburg and Stepanov 2014). Consider a magnetic field of Beltrami type, $\boldsymbol{B} = (\cos kz, -\sin kz, 0)$, write it in complex form as $\mathscr{B} = B_x + \mathrm{i}B_y$, so that $\mathscr{B}(z) = B_\parallel\, e^{\mathrm{i}\psi_B(z)}$ with $\psi_B(z) = kz$, and assume that ϕ is linear in z (which is the case when $n_e B_\parallel = \text{const}$). We thus obtain $\mathscr{B} = \mathscr{B}(\phi(z))$. The Faraday dispersion function is essentially given by $F(\phi) \propto \mathscr{B}^2$, so its phase is now $2\psi_B$ and one loses phase information, which is referred to as the π ambiguity. Inserting this into Eq. (19.15), one sees that most of the contribution to the integral comes from those values of λ^2 for which the phase is constant or “stationary”, i.e.,

$$2\mathrm{i}(\psi_B + \phi\lambda^2) = \text{const.} \tag{19.16}$$

Making use of the fact that for constant $n_e B_\parallel$ we have $\phi = -K n_e B_\parallel\, z$, and thus

$$\lambda^2 = -k/K n_e B_\parallel \tag{19.17}$$

is the condition for the wavelength for which the integral in Eq. (19.15) gets its largest contribution. Similar conditions have also been derived by Sokoloff et al. (1998) and Arshakian et al. (2011).

The Fourier transform of such a complex field would directly reflect the individual constituents of the magnetic field. For example, a superposition of two helical fields yields two corresponding peaks in the Fourier spectrum of $\mathscr{B}$; see Fig. 19.11c, where we have peaks at normalized Fourier variables $2\lambda^2/\lambda_0^2 = 1$ and -5. However, the quantity inferred by RM synthesis is the Faraday dispersion function, which is related to the square of $\mathscr{B}$, and its Fourier spectrum is more complicated; see Fig. 19.11d, where we have peaks at $2\lambda^2/\lambda_0^2 = 2, -4$, and -10. Thus, the two modes combine to a new one with a Fourier variable that is equal to the sum $1 + (-5) = -4$, with side lobes separated by their difference $1 - (-5) = 6$ to the left and the right. The corresponding modulus and phase ψ_B are shown in panels (a) and (b), respectively. Also shown is the phase ψ'_B, which is ψ_B remapped onto the range from $-\pi/2$ to $\pi/2$.

The magnetic fields of spiral galaxies are expected to be dominated by a strong toroidal component. This component might provide a reasonably uniform line-of-sight component without reversals when viewed edge-on. This would then provide an opportunity to detect polarization signatures from magnetic fields with different signs of magnetic helicity in different quadrants of the galaxy. Figure 19.12 provides a sketch with a line-of-sight component of different sign on the left or the right of the rotation axis. On the right, RM is positive (field points toward observer), so we can detect signatures of the field with positive helicity. Since the large-scale field has positive magnetic helicity in the upper disc plane, signatures from this component can be detected in quadrants I and III. Conversely, since the small-scale field has positive magnetic helicity in the lower disc plane, signatures from this component can be detected in quadrants II and IV.

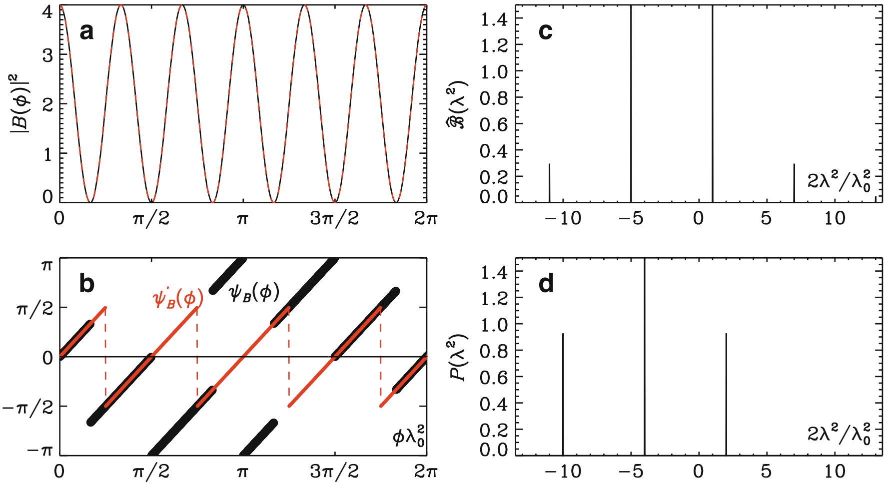

Fig. 19.11 (**a**) $|B|^2(\phi)$, (**b**) $\psi_B(\phi)$ and $\psi'_B(\phi)$, (**c**) $\mathscr{B}(k)$, and (**d**) $P(k)$ for a tri-helical magnetic field with $k_2/k_1 = -5$ using RM > 0. In panel (**b**), the *dashed blue lines* correspond to $\pi/2 - \phi|\lambda_1^2|$ and $3\pi/2 - \phi|\lambda_1^2|$ and mark the points where the phase of $\psi_B(\phi)$ jumps

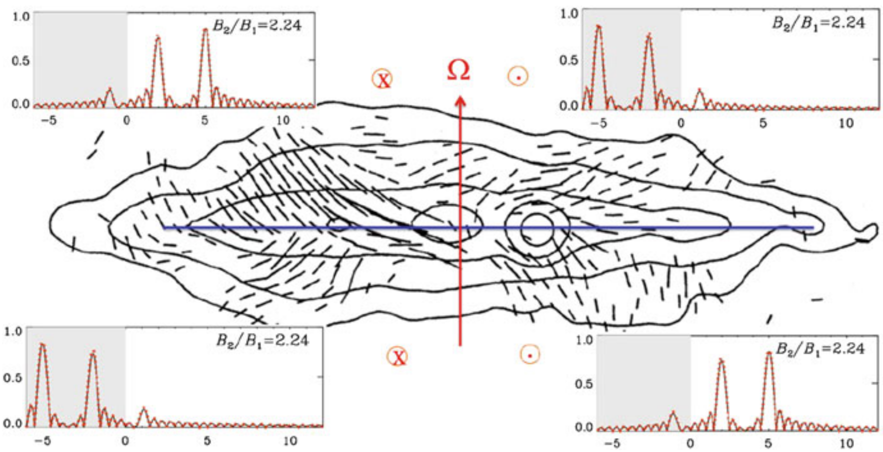

Fig. 19.12 Illustration of the four quadrants of an edge-one galaxy, where two are expected to show signatures fields of positive helicity and two signatures fields of negative helicity. The 2×2 panels correspond to polarization maps shown in Brandenburg and Stepanov (2014) for different signs of RM and helicity

19.5 Primordial Magnetic Field

Primordial magnetic fields are generated in the early Universe, either at inflation (Turner and Widrow 1988) at $\lesssim 10^{-32}$ s, the electroweak phase transition at $\sim 10^{-12}$ s, or the QCD phase transition at $\sim 10^{-6}$ s; see, for example, Vachaspati

(1991, 2001) and the review by Durrer and Neronov (2013). Such magnetic fields are basically subject to subsequent turbulent decay. Nevertheless, the evolution of these magnetic fields is essentially governed by the same hydromagnetic equations as those used to describe dynamos in galaxies, for example. The purpose of this section is to point out that there are some important similarities between decaying turbulence in the early Universe and (supernova-) driven turbulence in contemporary galaxies.

Especially for magnetic fields generated at the electroweak phase transition, there is the possibility that such fields are helical. This would then lead to an inverse cascade (Pouquet et al. 1976) and a transfer of magnetic energy to progressively larger scale or smaller wavenumbers; see Fig. 19.13, where we show magnetic energy spectra $E_{\rm M}$ versus wavenumber k and compare with the case where k is divided by the integral wavenumber $k_{\rm M}(t)$ defined through

$$k_{\rm M}^{-1}(t) = \int k^{-1} E_{\rm M}(k,t)\,{\rm d}k \Bigg/ \int E_{\rm M}(k,t)\,{\rm d}k. \qquad (19.18)$$

Simulations like those shown here are now done by several groups (Christensson et al. 2001; Banerjee and Jedamzik 2004; Kahniashvili et al. 2013). One of the main motivations for this work is the realization that magnetic fields generated at the time of the electroweak phase transition would now have a length scale of just one AU, which is short compared with the scale of galaxies. In fact, in the radiation dominated era, the hydromagnetic equations in an expanding universe can be rewritten in the usual form when using conformal time and suitably rescaled quantities; see Brandenburg et al. (1996), who then used a magnetic helicity-

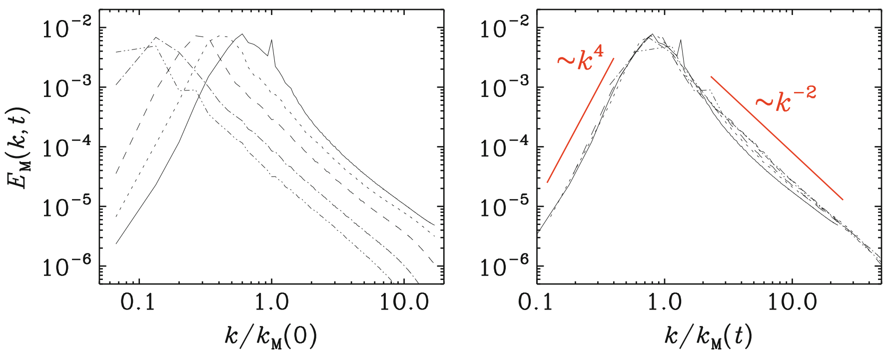

Fig. 19.13 Magnetic energy spectra at different times in the presence of magnetic helicity with $\mathrm{Pr}_M = 1$. On the right, the abscissa is rescaled by $k_{\rm M}(t)$, which make the spectra collapse onto each other. The Reynolds number based on the wavenumber $k_{\rm M}$ is around 1,000. The spike at k/k_0 corresponds to the driving scale prior to letting the field decay

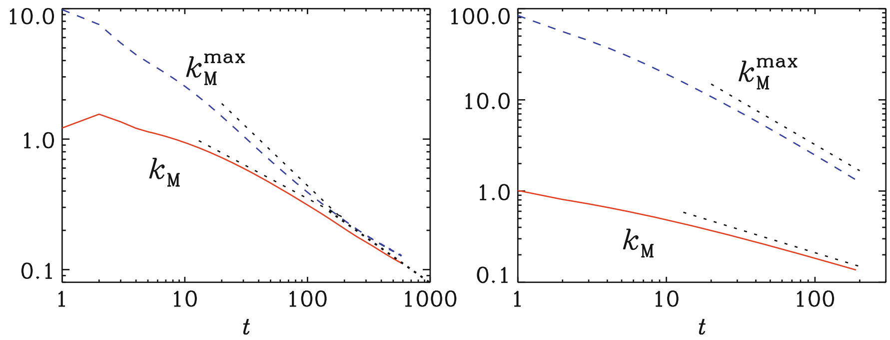

Fig. 19.14 Evolution of $k_{\rm M}(t)$ (*solid*) and $k_{\rm M}^{\rm max}(t)$ (*dashed*) for a fractional initial helicity (*left*) and zero initial helicity (*right*)

conserving cascade model of hydromagnetic turbulence to investigate the increase of the correlation length with time.

In reality, the magnetic field will never be fully helical. However, non-helical turbulence decays faster (like t^{-1}) than helical one (like $t^{-2/3}$); see Biskamp and Müller (1999). One can think of partially helical turbulence as a mixture of a more rapidly decaying nonhelical component and a less rapidly decaying helical component. After some time, the former one will have died out and so only the latter, helical component will survive. In Fig. 19.14 we show the scaling of $k_{\rm M}$ for a weakly helical and a nonhelical case and compare with the maximum possible value derived from the realizability condition, i.e.

$$k_{\rm M}(t) \leq k_{\rm M}^{\rm max}(t) \equiv 2\mathscr{E}(t)/|\mathscr{H}(t)|, \qquad (19.19)$$

where $\mathscr{E}(t) = \int E_{\rm M}(k,t)\,{\rm d}k$ and $\mathscr{H}(t) = \int H_{\rm M}(k,t)\,{\rm d}k$ are magnetic energy and helicity computed from the spectra. This was originally demonstrated by Tevzadze et al. (2012) using simulations similar to those presented here.

The decay of helical magnetic fields is also amenable to the mean-field treatment discussed in Sect. 19.3.3. Helicity from large-scale fields drives helicity at small scales via Eq. (19.13) and thereby an α effect through Eq. (19.11). This slows down the decay (Yousef and Brandenburg 2003; Kemel et al. 2011; Blackman and Subramanian 2013; Bhat et al. 2014) and may be relevant to the survival of galactic magnetic fields, as already mentioned in Sect. 19.2.2.

Remarkably, simulations have shown that some type of inverse cascading occurs also in the *absence* of magnetic helicity (Christensson et al. 2001; Kahniashvili et al. 2013). In Fig. 19.15 we show such a result from a simulation at a numerical resolution of 2304^3 meshpoints (Brandenburg and Stepanov 2014). However, the detailed reason for this inverse energy transfer still remains to be clarified.

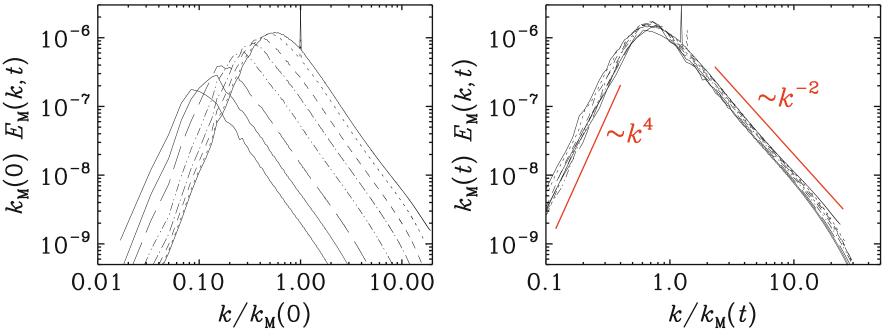

Fig. 19.15 Similar to Fig. 19.13, but for the case without initial helicity and initial scale separation ratio of the forcing of $k_{\rm min}/k_1 = 60$. $\mathrm{Pr}_M = 1$. On the right, the ordinate is scaled with $k_{\rm M}(t)$, in addition to the scaling of the abscissa with $1/k_{\rm M}(t)$

Conclusion

The overall significance of primordial magnetic fields is still unclear, because contemporary magnetic fields might well have been produced by some type of dynamo within bodies such as stars and accretion discs within galaxies, and would then have been ejected into the rest of the gas outside. Whether such mechanisms would be sufficiently powerful to explain magnetic fields even between clusters of galaxies remains to be seen. In this connection it is noteworthy that Neronov and Vovk (2010) found a lower bound on the magnetic field strength of 3×10^{-16} G based on the non-detection of GeV gamma-ray emission from the electromagnetic cascade of TeV gamma rays in the intergalactic medium. This bound is well above the even rather optimistic earlier estimated galactic seed magnetic field strengths (Rees 1987).

Invoking some type of large-scale seed magnetic field seems to be the only plausible option if one wants to explain the non-axisymmetric magnetic fields in M81. However, this galaxy is perhaps only one of the few where there is still strong evidence for the existence of a non-axisymmetric magnetic field. In agreement with mean-field dynamo theory, most galaxies harbor axisymmetric magnetic fields and their toroidal field is symmetric about the midplane.

With the help of turbulent dynamo simulations over the past 20 years, it is now clear that the conventional $\alpha\Omega$ type dynamo must produce large-scale magnetic fields that have two different signs of helicity, one at large scales and the opposite one at small scales. Such magnetic fields are called bi-helical and might be detectable through their specific signature in polarized radio emission. These are some of the aspects that we have highlighted in the present review about galactic dynamo simulations. Clearly, simulations have

(continued)

to be conducted in close comparison with theory. By now, simulations have reached sufficiently high magnetic Reynolds numbers that simple theories such as first-order smoothing clearly break down and some kind of asymptotic regime commences. Given that it will not be possible to reach asymptotic scaling yet, is must eventually be the interplay between simulations and theory that can provide a meaningful understanding of galactic magnetism.

Acknowledgements I am indebted to Oliver Gressel and Kandaswamy Subramanian for reading the manuscript and providing help and useful comments. Financial support from the European Research Council under the AstroDyn Research Project 227952, the Swedish Research Council under the grants 621-2011-5076 and 2012-5797, as well as the Research Council of Norway under the FRINATEK grant 231444 are gratefully acknowledged.

References

Arshakian, T.G., Beck, R.: Optimum frequency band for radio polarization observations. Monthly Notices Roy. Astron. Soc. **418**, 2336–2342 (2011)

Banerjee, R., Jedamzik, K.: Evolution of cosmic magnetic fields: from the very early Universe, to recombination, to the present. Phys. Rev. D **70**, 123003 (2004)

Beck, R.: Magnetism in the spiral galaxy NGC 6946: magnetic arms, depolarization rings, dynamo modes, and helical fields. Astron. Astrophys. **470**, 539–556 (2007)

Beck, R., Brandenburg, A., Moss, D., Shukurov, A., Sokoloff, D.: Galactic magnetism: recent developments and perspectives. Ann. Rev. Astron. Astrophys. **34**, 155–206 (1996)

Beck, R., Wielebinski, R.: Magnetic fields in galaxies, In: Oswalt, T.D., Gilmore, G. (eds.) Planets, Stars and Stellar Systems, vol. 5, pp. 641–723. Springer Science+Business Media, Dordrecht (2013)

Bhat, P., Blackman, E.G., Subramanian, K.: Resilience of helical fields to turbulent diffusion II: direct numerical simulations. Monthly Notices Roy. Astron. Soc. **438**, 2954–2966 (2014)

Biskamp, D., Müller, W.-C.: Decay laws for three-dimensional magnetohydrodynamic turbulence. Phys. Rev. Lett. **83**, 2195–2198 (1999)

Blackman, E.G., Brandenburg, A.: Dynamic nonlinearity in large scale dynamos with shear. Astrophys. J. **579**, 359–373 (2002)

Blackman, E.G., Field, G.B.: Constraints on the magnitude of α in dynamo theory. Astrophys. J. **534**, 984–988 (2000)

Blackman, E.G., Subramanian, K.: On the resilience of helical magnetic fields to turbulent diffusion and the astrophysical implications. Monthly Notices Roy. Astron. Soc. **429**, 1398–1406 (2013)

Brandenburg, A.: Disc turbulence and viscosity. In: Abramowicz, M.A., Björnsson, G., Pringle, J.E. (eds.) Theory of Black Hole Accretion Discs, pp. 61–86. Cambridge University Press, Cambridge (1998)

Brandenburg, A.: Chandrasekhar-Kendall functions in astrophysical dynamos. Pramana J. Phys. **77**, 67–76 (2011)

Brandenburg, A., Dobler, W., Subramanian, K.: Magnetic helicity in stellar dynamos: new numerical experiments. Astron. Nachr. **323**, 99–122 (2002)

Brandenburg, A., Enqvist, K., Olesen, P.: Large-scale magnetic fields from hydromagnetic turbulence in the very early universe. Phys. Rev. D **54**, 1291–1300 (1996)

Brandenburg, A., Käpylä, P.J., Mohammed, A.: Non-Fickian diffusion and tau-approximation from numerical turbulence. Phys. Fluids **16**, 1020–1027 (2004)
Brandenburg, A., Nordlund, A.A.: Astrophysical turbulence modeling. Rep. Prog. Phys. **74**, 046901 (2011)
Brandenburg, A., Rädler, K.-H., Rheinhardt, M., Subramanian, K.: Magnetic quenching of alpha and diffusivity tensors in helical turbulence. Astrophys. J. Lett. **687**, L49–L52 (2008a)
Brandenburg, A., Rädler, K.-H., Schrinner, M.: Scale dependence of alpha effect and turbulent diffusivity. Astron. Astrophys. **482**, 739–746 (2008b)
Brandenburg, A., Sandin, C.: Catastrophic alpha quenching alleviated by helicity flux and shear. Astron. Astrophys. **427**, 13–21 (2004)
Brandenburg, A., Stepanov, R.: Faraday signature of magnetic helicity from reduced depolarization. Astrophys. J. **786**, 91 (2014)
Brandenburg, A., Subramanian, K., Balogh, A., Goldstein, M.L.: Scale-dependence of magnetic helicity in the solar wind. Astrophys. J. **734**, 9 (2011)
Brandenburg, A., Tuominen, I., Rädler, K.-H.: On the generation of non-axisymmetric magnetic fields in mean-field dynamos. Geophys. Astrophys. Fluid Dyn. **49**, 45–55 (1989)
Brentjens, M.A., de Bruyn, A.G.: Faraday rotation measure synthesis. Astron. Astrophys. **441**, 1217–1228 (2005)
Burn, B.J.: On the depolarization of discrete radio sources by Faraday dispersion. Monthly Notices Roy. Astron. Soc. **133**, 67–83 (1966)
Candelaresi, S., Brandenburg, A.: How much helicity is needed to drive large-scale dynamos? Phys. Rev. E **87**, 043104 (2013)
Cattaneo, F., Vainshtein, S.I.: Suppression of turbulent transport by a weak magnetic field. Astrophys. J. Lett. **376**, L21–L24 (1991)
Chamandy, L., Subramanian, K., Shukurov, A.: Galactic spiral patterns and dynamo action— I. A new twist on magnetic arms. Monthly Notices Roy. Astron. Soc. **428**, 3569–3589 (2013)
Chamandy, L., Subramanian, K., Quillen, A.: Magnetic arms generated by multiple interfering galactic spiral patterns. Monthly Notices Roy. Astron. Soc. **437**, 562–574 (2014)
Christensson, M., Hindmarsh, M., Brandenburg, A.: Inverse cascade in decaying 3D magnetohydrodynamic turbulence. Phys. Rev. E **64**, 056405-6 (2001)
Del Sordo, F., Brandenburg, A.: Vorticity production through rotation, shear, and baroclinicity. Astron. Astrophys. **528**, A145 (2011)
Del Sordo, F., Guerrero, G., Brandenburg, A.: Turbulent dynamo with advective magnetic helicity flux. Monthly Notices Roy. Astron. Soc. **429**, 1686–1694 (2013)
Donner, K.J., Brandenburg, A.: Generation and interpretation of galactic magnetic fields. Astron. Astrophys. **240**, 289–298 (1990)
Durrer, R., Neronov, A.: Cosmological magnetic fields: their generation, evolution and observation. Astron. Astrophys. Rev. **21**, 62 (2013)
Ferrière, K.: Effect of an ensemble of explosions on the galactic dynamo. I. General formulation. Astrophys. J. **389**, 286–296 (1992)
Ferrière, K.: The full alpha-tensor due to supernova explosions and superbubbles in the galactic disk. Astrophys. J. **404**, 162–184 (1993)
Frick, P., Sokoloff, D., Stepanov, R., Beck, R.: Faraday rotation measure synthesis for magnetic fields of galaxies. Monthly Notices Roy. Astron. Soc. **414**, 2540–2549 (2011)
Gent, F.A., Shukurov, A., Fletcher, A., Sarson, G.R., Mantere, M.J.: The supernova-regulated ISM—I. The multiphase structure. Monthly Notices Roy. Astron. Soc. **432**, 1396–1423 (2013a)
Gent, F.A., Shukurov, A., Sarson, G.R., Fletcher, A., Mantere, M.J.: The supernova-regulated ISM—II. The mean magnetic field. Monthly Notices Roy. Astron. Soc. **430**, L40–L44 (2013b)
Gießübel, R., Heald, G., Beck, R., Arshakian, T.G.: Polarized synchrotron radiation from the Andromeda galaxy M 31 and background sources at 350 MHz. Astron. Astrophys. **559**, A27 (2013)
Gissinger, C., Fromang, S., Dormy, E.: Direct numerical simulations of the galactic dynamo in the kinematic growing phase. Monthly Notices Roy. Astron. Soc. **394**, L84–L88 (2009)

Gressel, O., Elstner, D., Ziegler, U., Rüdiger, G.: Direct simulations of a supernova-driven galactic dynamo. Astron. Astrophys. **486**, L35–L38 (2008a)
Gressel, O., Ziegler, U., Elstner, D., Rüdiger, G.: Dynamo coefficients from local simulations of the turbulent ISM. Astron. Nachr. **329**, 619–624 (2008b)
Gressel, O., Elstner, D., Ziegler, U.: Towards a hybrid dynamo model for the Milky Way. Astron. Astrophys. **560**, A93 (2013)
Gruzinov, A.V., Diamond, P.H.: Self-consistent theory of mean-field electrodynamics. Phys. Rev. Lett. **72**, 1651–1653 (1994)
Hanasz, M., Kowal, G., Otmianowska-Mazur, K., Lesch, H.: Amplification of galactic magnetic fields by the cosmic-ray-driven dynamo. Astrophys. J. **605**, L33–L36 (2004)
Hanasz, M., Otmianowska-Mazur, K., Kowal, G., Lesch, H.: Cosmic-ray-driven dynamo in galactic disks. A parameter study. Astron. Astrophys. **498**, 335–346 (2009)
Heald, G., Braun, R., Edmonds, R.: The Westerbork SINGS survey. II Polarization, Faraday rotation, and magnetic fields. Astron. Astrophys. **503**, 409–435 (2009)
Hubbard, A., Brandenburg, A.: Memory effects in turbulent transport. Astrophys. J. **706**, 712–726 (2009)
Hubbard, A., Brandenburg, A.: Magnetic helicity fluxes in an α^2 dynamo embedded in a halo. Geophys. Astrophys. Fluid Dyn. **104**, 577–590 (2010)
Hubbard, A., Brandenburg, A.: Catastrophic quenching in $\alpha\Omega$ dynamos revisited. Astrophys. J. **748**, 51 (2012)
Jansson, R., Farrar, G.R.: A new model of the Galactic magnetic field. Astrophys. J. **757**, 14 (2012)
Kahniashvili, T., Tevzadze, A.G., Brandenburg, A., Neronov, A.: Evolution of primordial magnetic fields from phase transitions. Phys. Rev. D **87**, 083007 (2013)
Kemel, K., Brandenburg, A., Ji, H.: A model of driven and decaying magnetic turbulence in a cylinder. Phys. Rev. E **84**, 056407 (2011)
Kleeorin, N.I., Ruzmaikin, A.A.: Dynamics of the average turbulent helicity in a magnetic field. Magnetohydrodynamics **18**, 116–122 (1982). Translation from Magnitnaya Gidrodinamika **2**, 17–24 (1982)
Knobloch, E.: Turbulent diffusion of magnetic fields. Astrophys. J. **225**, 1050–1057 (1978)
Korpi, M.J., Brandenburg, A., Shukurov, A., Tuominen, I., Nordlund, A.A.: A supernova regulated interstellar medium: simulations of the turbulent multiphase medium. Astrophys. J. Lett. **514**, L99–L102 (1999)
Korpi, M.J., Brandenburg, A., Tuominen, I.: Driving interstellar turbulence by supernova explosions. Studia Geophys. et Geod. **42**, 410–418 (1998)
Krause, M., Beck, R., Hummel, E.: The magnetic field structures in two nearby spiral galaxies. II. The bisymmetric spiral field in M81. Astron. Astrophys. **217**, 17–30 (1989)
Krause, F., Rädler, K.-H.: Mean-field Magnetohydrodynamics and Dynamo Theory. Pergamon Press, Oxford (1980)
Kulpa-Dybeł, K., Otmianowska-Mazur, K., Kulesza-Żydzik, B., Hanasz, M., Kowal, G., Wóltański, D., Kowalik, K.: Global simulations of the magnetic field evolution in barred galaxies under the influence of the cosmic-ray-driven dynamo. Astrophys. J. Lett. **733**, L18 (2011)
Layzer, D., Rosner, R., Doyle, H.T.: On the origin of solar magnetic fields. Astrophys. J. **229**, 1126–1137 (1979)
Mestel, L., Subramanian, K.: Galactic dynamos and density wave theory. Monthly Notices Roy. Astron. Soc. **248**, 677–687 (1991)
Mitra, D., Candelaresi, S., Chatterjee, P., Tavakol, R., Brandenburg, A.: Equatorial magnetic helicity flux in simulations with different gauges. Astron. Nachr. **331**, 130–135 (2010)
Moffatt, H.K.: Magnetic Field Generation in Electrically Conducting Fluids. Cambridge University Press, Cambridge (1978)
Moss, D.: Modelling magnetic fields in spiral galaxies. Astron. Geophys. **53**, 23–28 (2012)
Moss, D., Brandenburg, A., Tuominen, I.: Properties of mean field dynamos with nonaxisymmetric α-effect. Astron. Astrophys. **247**, 576–579 (1991)

Moss, D., Brandenburg, A., Donner, K.J., Thomasson, M.: Models for the magnetic field of M81. Astrophys. J. **409**, 179–189 (1993)
Moss, D., Beck, R., Sokoloff, D., Stepanov, R., Krause, M., Arshakian, T.G.: The relation between magnetic and material arms in models for spiral galaxies. Astron. Astrophys. **556**, A147 (2013)
Neronov, A., Vovk, I.: Evidence for strong extragalactic magnetic fields from Fermi observations of TeV blazars. Science **328**, 73–192 (2010)
Parker, E.N.: Hydromagnetic dynamo models. Astrophys. J. **122**, 293–314 (1955)
Parker, E.N.: The generation of magnetic fields in astrophysical bodies. II. The galactic field. Astrophys. J. **163**, 255–278 (1971)
Parker, E.N.: Fast dynamos, cosmic rays, and the galactic magnetic field. Astrophys. J. **401**, 137–145 (1992)
Piddington, J.H.: Turbulent diffusion of magnetic fields in astrophysical plasmas. Astrophys. J. **247**, 293–299 (1981)
Pouquet, A., Frisch, U., Léorat, J.: Strong MHD helical turbulence and the nonlinear dynamo effect. J. Fluid Mech. **77**, 321–354 (1976)
Rädler, K.-H.: Mean field approach to spherical dynamo models. Astron. Astrophys. **301**, 101–129 (1980)
Rädler, K.-H.: Investigations of spherical kinematic mean-field dynamo models. Astron. Nachr. **307**, 89–113 (1986a)
Rädler, K.-H.: On the effect of differential rotation on axisymmetric and non-axisymmetric magnetic fields of cosmical bodies. Plasma Phys. **ESA SP-251**, 569–574 (1986b)
Rees, M.J.: The origin and cosmogonic implications of seed magnetic fields. Quart. J. Roy. Astron. Soc. **28**, 197–206 (1987)
Rheinhardt, M., Brandenburg, A.: Test-field method for mean-field coefficients with MHD background. Astron. Astrophys. **520**, A28 (2010)
Rheinhardt, M., Brandenburg, A.: Modeling spatio-temporal nonlocality in mean-field dynamos. Astron. Nachr. **333**, 71–77 (2012)
Ruzmaikin, A.A., Sokolov, D.D., Shukurov, A.M.: Magnetic field distribution in spiral galaxies. Astron. Astrophys. **148**, 335–343 (1985)
Ruzmaikin, A.A., Sokoloff, D.D., Shukurov, A.M.: Magnetic Fields of Galaxies. Kluwer Academic Publishers, Dordrecht (1988)
Schrinner, M., Rädler, K.-H., Schmitt, D., Rheinhardt, M., Christensen, U.: Mean-field view on rotating magnetoconvection and a geodynamo model. Astron. Nachr. **326**, 245–249 (2005)
Schrinner, M., Rädler, K.-H., Schmitt, D., Rheinhardt, M., Christensen, U.R.: Mean-field concept and direct numerical simulations of rotating magnetoconvection and the geodynamo. Geophys. Astrophys. Fluid Dyn. **101**, 81–116 (2007)
Shukurov, A.: Mesoscale magnetic structures in spiral galaxies. In: Wielebinski, R., Beck, R. (eds.) Cosmic Magnetic Fields. Lect. Notes Phys., vol. 664, pp. 113–135. Springer, Berlin (2005)
Shukurov, A., Sokoloff, D., Subramanian, K., Brandenburg, A.: Galactic dynamo and helicity losses through fountain flow. Astron. Astrophys. **448**, L33–L36 (2006)
Snodin, A.P., Brandenburg, A., Mee, A.J., Shukurov, A.: Simulating field-aligned diffusion of a cosmic ray gas. Monthly Notices Roy. Astron. Soc. **373**, 643–652 (2006)
Sofue, Y., Fujimoto, M., Wielebinski, R.: Global structure of magnetic fields in spiral galaxies. Ann. Rev. Astron. Astrophys. **24**, 459–497 (1986)
Sokoloff, D.D., Bykov, A.A., Shukurov, A., Berkhuijsen, E.M., Beck, R., Poezd, A.D.: Depolarization and Faraday effects in galaxies. Monthly Notices Roy. Astron. Soc. **299**, 189–206 (1998)
Steenbeck, M., Krause, F.: Zur Dynamotheorie stellarer und planetarer Magnetfelder I. Berechnung sonnenähnlicher Wechselfeldgeneratoren. Astron. Nachr. **291**, 49–84 (1969a)
Steenbeck, M., Krause, F.: Zur Dynamotheorie stellarer und planetarer Magnetfelder II. Berechnung planetenähnlicher Gleichfeldgeneratoren. Astron. Nachr. **291**, 271–286 (1969b)
Steenbeck, M., Krause, F., Rädler, K.-H.: Berechnung der mittleren Lorentz-Feldstärke $\overline{\boldsymbol{v} \times \boldsymbol{B}}$ für ein elektrisch leitendes Medium in turbulenter, durch Coriolis-Kräfte beeinflußter Bewegung. Z. Naturforsch. **21a**, 369–376 (1966). See also the translation in Roberts & Stix, The turbulent dynamo, Tech. Note 60, NCAR, Boulder, Colorado (1971)

Subramanian, K., Brandenburg, A.: Nonlinear current helicity fluxes in turbulent dynamos and alpha quenching. Phys. Rev. Lett. **93**, 205001 (2004)

Subramanian, K., Brandenburg, A.: Magnetic helicity density and its flux in weakly inhomogeneous turbulence. Astrophys. J. **648**, L71–L74 (2006)

Subramanian, K., Mestel, L.: Galactic dynamos and density wave theory—II. An alternative treatment for strong non-axisymmetry. Monthly Notices Roy. Astron. Soc. **265**, 649–654 (1993)

Sur, S., Shukurov, A., Subramanian, K.: Galactic dynamos supported by magnetic helicity fluxes. Monthly Notices Roy. Astron. Soc. **377**, 874–882 (2007)

Tevzadze, A.G., Kisslinger, L., Brandenburg, A., Kahniashvili, T.: Magnetic fields from QCD phase transitions. Astrophys. J. **759**, 54 (2012)

Thomasson, M., Donner, K.J.: A model of the tidal interaction between M81 and NGC3077. Astron. Astrophys. **272**, 153–160 (1993)

Turner, M.S., Widrow, L.M.: Inflation-produced, large-scale magnetic fields. Phys. Rev. D **37**, 2743–2754 (1988)

Vachaspati, T.: Magnetic fields from cosmological phase transitions. Phys. Lett. B **265**, 258–261 (1991)

Vachaspati, T.: Estimate of the primordial magnetic field helicity. Phys. Rev. Lett. **87**, 251302 (2001)

Vainshtein, S.I., Cattaneo, F.: Nonlinear restrictions on dynamo action. Astrophys. J. **393**, 165–171 (1992)

Vainshtein, S.I., Ruzmaikin, A.A.: Generation of the large-scale Galactic magnetic field. Sov. Astron. **16**, 365–367 (1971)

Vishniac, E.T., Cho, J., Magnetic helicity conservation and astrophysical dynamos. Astrophys. J. **550**, 752–760 (2001)

Warnecke, J., Brandenburg, A., Mitra, D.: Magnetic twist: a source and property of space weather. J. Spa. Weather Spa. Clim. **2**, A11 (2012)

Yousef, T.A., Brandenburg, A.: Relaxation of writhe and twist of a bi-helical magnetic field. Astron. Astrophys. **407**, 7–12 (2003)